Comparative analysis of three different types of self-healing concrete via permeability testing and a quasi-steady-state chloride migration test

Laurena De Brabandere[1+], Tim Van Mullem[1+], Jung Hwan Lee[2], Jung-Il Suh[3], Kwang-Myong Lee[2], Nele De Belie[1]

[1] Magnel-Vandepitte Laboratory, Department of Structural Engineering and Building Materials, Faculty of Engineering and Architecture, Ghent University, Technologiepark Zwijnaarde 60, B-9052 Gent, Belgium

[2] Department of Civil, Architectural and Environmental System Engineering, Sungkyunkwan University, Suwon 16419, Korea

[3] Construction Technology Center, Korea Conformity Laboratories, Seoul, 08053, Korea

[+] These authors contributed equally to this publication.

Corresponding author: nele.debelie@ugent.be

Abstract

Concrete is the most used construction material in the world and with the growing world population, the demand for housing and infrastructure keeps increasing. Due to its low tensile strength, concrete cracks easily and these cracks have a negative effect on the durability. Different studies have already been conducted on the development of self-healing concrete, which has the ability to heal its own cracks. Unfortunately, due to a lack of standardized test methods, the boundary conditions in these studies are often different, making it difficult to do an accurate comparison. In this research, three different healing agents are tested using the same test methods under the same boundary conditions: a powder of organic/inorganic composite material (WM), solidified calcium sulfoaluminate capsules (SMU) and bacterial pellets (KU). The healing efficiency of the agents is tested with (1) a low-head water flow test on prismatic specimens cracked in a three-point bending test with subsequent active crack width control, (2) a Korean water permeability test on cylindrical specimens cracked by a Brazilian splitting test, (3) a chloride diffusion test and (4) a quasi-steady-state chloride migration test. The results showed that WM performed superior with respect to the reference mix and the other healing agents in the two water permeability tests and the quasi-steady-state chloride migration. The performance of SMU and KU was depending on the healing condition. When fully saturated during healing, the KU specimens had a good behaviour and SMU performed poorly. For the cylindrical specimens, with the specimen partly immersed in water, SMU and KU had a similar performance which was better in comparison to the reference.

Keywords: self-healing concrete; water permeability; chloride diffusion; quasi-steady-state chloride migration; active crack width control.

1. Introduction

With the world population growing beyond eight billion people the demand for housing and infrastructure keeps increasing. Concrete is the most used construction material in the world due to its high compressive strength, its low cost, and its freedom of form. However, the production of concrete is directly linked to the production of cement which has a high environmental burden. The Intergovernmental Panel on Climate Change (IPCC) assessed that buildings constitute 21% of the

Global greenhouse gasses (construction process and energy demand during operation) [1]. This can be divided in 57% coming from indirect emissions for offsite generation of electricity and heat, 24% coming from direct emission on site, and 18% coming from the use of cement and steel. These numbers clearly highlight the large quantity of greenhouse gasses which are linked to the construction process.

Due to the limited tensile strength, concrete cracks easily and these cracks have a negative effect on the durability, limiting the service life. More than a decade, researchers have been developing different types of self-healing concrete [2]. Self-healing concrete is able to repair its own cracks. As such, cracks can be repaired starting from the moment that they are formed, and it is not needed to wait for a maintenance intervention as is the case for traditional concrete. The crack repair has a positive effect on the durability which can allow the service life to be extended. Thus, structures can operate for a longer time without the need to replace them. This results in an improved material efficiency. Using materials more thoughtfully and in an efficient way has been identified as one of the ways to reach net zero emissions from greenhouse gasses by 2050 [1].

The ingress of chloride ions in concrete is one of the most important causes of steel reinforcement corrosion [3]. Due to the presence of cracks, chloride ions can migrate faster into the concrete up to the level of the reinforcement. Corrosion measurements are often time consuming and difficult. Therefore, the resistance against chloride penetration is often measured through chloride diffusion and chloride migration tests. Chloride migration tests have the advantage of providing a fast way to calculate a diffusion or migration coefficient, while diffusion tests usually take a couple of months. There are different migration tests available. Rapid chloride migration (RCM) is a test method that calculates a coefficient from non-steady-state migration [4]. On the contrary, during the migration test based on ASTM C1202, the migration coefficient is calculated from measurements during a steady-state regime [5].

Different self-healing methods have been developed, such as: microbially induced calcium carbonate precipitation [6], reactive agents like polymers or minerals that are micro- or macro-encapsulated [7], [8], or supplied by vascular networks [9], [10], stimulated autogenous healing by superabsorbent polymers [11] and crystalline admixtures [12]. The healing agents used in this research are either bacteria-based or consist of organic/inorganic composite powder or encapsulated minerals that stimulate the autogenous healing of the concrete.

Depending on the healing agent and the institute which performs the test there can be a big difference in the boundary conditions (cracking age, healing conditions, healing duration,…) and the applied test method [13]. Hence, despite the large quantity of studies on self-healing of cementitious materials, it is often difficult to effectively compare the efficiency of different self-healing agents. The major contribution of this paper is that it tests three different healing agents with the same test methods under the same boundary conditions to establish the most suitable healing agents for a regain in liquid tightness with a possible application in a chloride-rich environment. The three different healing agents which are considered are: a powder of organic/inorganic composite material [14], solidified calcium sulfoaluminate capsules [15] and bacterial pellets [16].

To assess the performance of healing agents with regards to a regain in liquid tightness, permeability tests are commonly employed. Compared to visual crack closure measured by a microscope, which only evaluates closure at the crack mouth, they give an indication of the healing in the interior of the crack. It is for example possible that a crack seems visually closed, while water is still able to leak from the crack. The opposite situation is also possible; specimens with a limited visual crack closure could have no water leakage due to interior healing of the crack which is not visible at the crack mouth (the addition of superabsorbent particles (SAPs) for example can result in an immediate sealing effect due to the swelling of the SAPs [17, 18]). Compared to capillary absorption tests, permeability tests have the clear advantage that the measured flow rate is strongly dependent on the crack width [19] -and thus crack closure due to healing, while the relation between crack closure and capillary absorption is far less pronounced [20, 21]. The two methods which were employed in this study were chosen because they have already undergone a standardization process or at least have been studied via inter-laboratory testing. In addition, the pre-cracking method is different for the two employed methods. The first method consisted of a low-head water flow test on prismatic specimens cracked in a three-point bending test with subsequent active crack width control, because it has been identified that small changes in crack width can result in significant differences with respect to water flow through a crack [22]. To test the stability of the formed healing products at higher water pressures, a high-head water flow test (up until 2 bar) was executed on these specimens [18, 23].In the second method cylindrical specimens with the different agents were cracked in a Brazilian splitting test creating specimens with a different crack geometry, i.e. cracks with a constant thickness over the height instead of the more triangular shaped cracks in the prismatic specimens. These cylindrical specimens' healing was evaluated over time in a Korean water permeability test [24, 25]. After the healing period, these specimens were subjected to a chloride diffusion test. The performance with regards to chloride ingress after different healing periods was also evaluated by a quasi-steady-state chloride migration test for the reference specimens and the specimens containing the organic/inorganic composite material [5]. It is stressed that his paper does not try to establish the best testing method. After all, this is application-dependent because the best testing method is the one which represents the envisioned practical application the best and mimics the practical boundary conditions (as these are known to affect the healing performance [13]).

2. Materials

In this research 3 different healing agents (WM, KU and SMU) with different healing mechanisms are used which were all developed within the Korean based SHGC consortium. The agents have been individually tested and optimized in previous research [14-16]. These healing agents were selected due to the different approach that is used during the production of the agents and in the healing process when added to concrete, as it is rare to find a study which evaluates agents with a different healing mechanism. Two of the healing agents, KU and SMU, are encapsulated or pelletized to ensure healing of cracks that occur at a long-term age. Below the composition and production of the healing agents is explained.

2.1. Organic/inorganic composite material (WM)

An organic-inorganic composite material has been developed to self-heal cementitious systems. This healing agent is denoted WM. It is produced through a mechanochemical process (MCP) by mixing mainly MgO-CaO (approximately 60 %) as an expansion material, carbon, amorphous silica and an alkali activator. MgO-CaO has been widely used as a self-healing agent due to its expansive properties [26, 27]. The main hydration products of MgO and CaO are $Mg(OH)_2$ and portlandite ($Ca(OH)_2$) which have crystal forming properties and can therefore contribute to the self-healing of concrete. MCP is a powder processing technique where particles have repeated collisions in a ball mill in order to deform, fracture and cold weld the particles [28]. The application of MCP increases the reactivity of materials. The mechanochemical method is applied to induce mechanical and chemical bonding reactions of the constituents [14]. The average grain size is 45 ± 5 µm.

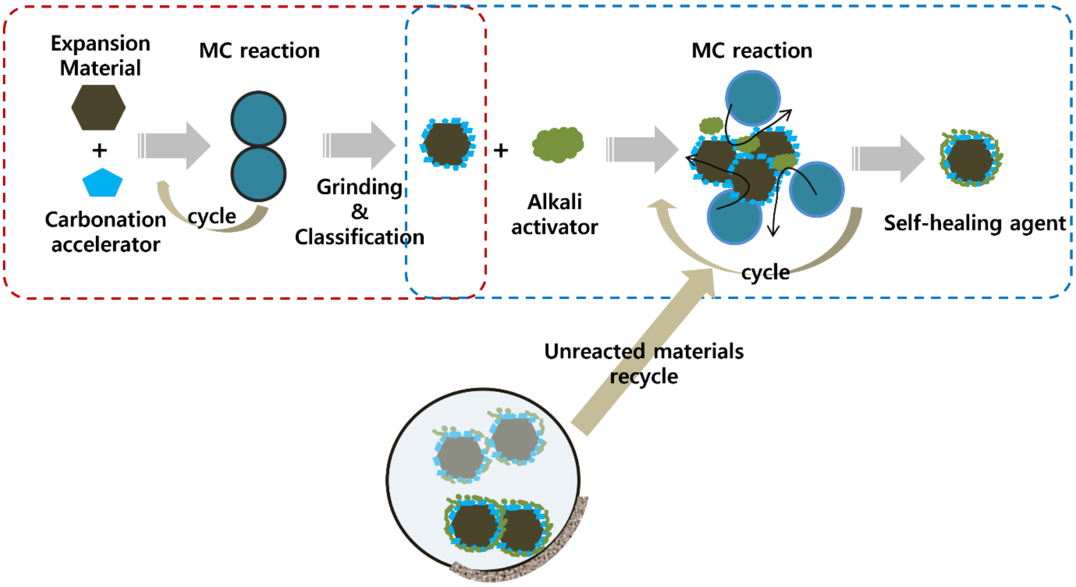

Figure 1: Production process of the WM organic-inorganic composite material by two mechanochemical (MC) processes. Adapted from [14].

2.2. Solidified calcium sulfoaluminate capsules (SMU)

Another self-healing material used in this research are capsules with a size from 0.85 to 1.2 mm containing an inorganic reactive powder. This inorganic powder consists out of calcium sulfoaluminate (CSA), which is an expansive material, and anhydrite ($CaSO_4$). When a crack is formed in the self-healing concrete containing the capsules, the inorganic powder comes in contact with water and ettringite and calcium hydroxide ($Ca(OH)_2$) are formed as healing products by a hydration reaction. The production process of these capsules consists out of the mixing and granulating of the healing materials and the coating of the reactive powder by spraying polyurethane [15]. The encapsulation and coating of the powder ensures that it can heal cracks that occur at a later age.

2.3. Bacterial pellet (KU)

The self-healing agent KU consists of pellets containing bacteria. For this, cocultured spray-dried bacteria powder is mixed into methylcellulose-based pellets. As bacteria, the *Lysinibacillus Boronitolerans* YS11 and *Bacillus Alkaliphilus* AK13 strains were used. The bacteria were cultured separately in Luria-Bertani (LB) medium. The composition of the LB medium is as follows: 0.5 % yeast extract, 1 % tryptone and 1 % sodium chloride. Then, the bacteria were inoculated and dried through a spray dryer [29]. The binder of these pellets mainly consists out of methylcellulose (MC), but also microcrystalline cellulose (MCC) is added as a binder to increase the particle's strength. Silicon dioxide (SiO_2) and diatomaceous earth (DE) are both used as a filler, SiO_2 as an inert filler, DE has the ability to absorb bacteria and nutrients on its surface. Besides the cocultured bacteria, also calcium lactate pentahydrate and yeast extract are added as nutrients. The manufactured pellets are small cylinders with a diameter of 2 mm and a length of 2-4 mm [16]. Pelletizing the bacteria protects the bacterial spores and ensures healing of cracks that occur in the long term. The addition of the MC pellets into concrete contributes to self-healing by three different mechanisms. First, the pellets can swell to 2.6 times their original volume when they come in contact with water and therefore, block the crack and reduce the flow of liquid through the crack. Second, the introduction of the pellets, which have a low strength in comparison to the paste and aggregates, changes the characteristics and the surface of the formed cracks. The environment in the crack changes, causing a reduced flow of liquid into the crack. Last, calcium carbonate is precipitated by the bacteria in the pellets by consuming nutrients available in the environment [16].

3. Test methods

3.1. Mortar composition and casting

Four different mortar mixes were made: (1) a mix containing the organic/inorganic hybrid material, referred to as WM, (2) a mix containing solidified calcium sulfoaluminate capsules, referred to as SMU, (3) a mix containing bacterial pellets, referred to as KU, and (4) a reference mix without any healing agents, named REF. Table 1 gives the mortar mix compositions. Note that the dosage of healing agents is based on previous research considering the healing performance and cost competitiveness.

Cylinders (height 200 mm, diameter 100 mm) and prisms (40 mm x 40 mm x 160 mm) were cast with each mix. All specimens per mix were cast from the same batch of mortar. A well-oiled smooth steel bar (Ø 5 mm) was positioned in the centre along the longitudinal axis with its centre 15 mm above the bottom of the prismatic moulds. After a day in the curing room (20 °C, > 95% RH), the specimens were demoulded. At this point the steel bar was pulled out of the prismatic specimens creating a cast-in hole along their length. The specimens were subsequently again stored in the curing room until cracking. At an age of 21 days, the cylinders were cut into 3 specimens with a height of 50 mm.

Table 1. Mortar mix composition.

Materials	REF	WM	SMU	KU	unit
CEM I 52.5 N	683	683	683	683	kg/m³
Sand 0-4 mm	1366	1333	1333	1346	kg/m³
Water	273	273	273	273	kg/m³
WM	-	5	-	-	m% of cement
SMU	-	-	5	-	m% of cement
KU	-	-	-	3	m% of cement

3.2. Fresh properties and strength

After mixing, the consistency of the fresh mixes was tested with a flow test according to EN 1015–3 [30], the table was not lubricated with oil but with a damp cloth. The flexural and compressive strength was tested on 3 mortar prisms (40 x 40 x 160 mm^3) at 7 and 28 days according to EN 196-1 [31].

3.3. Permeability testing

Two different permeability test methods were considered: one on prismatic specimens (using an active crack width control) and one on cylindrical specimens (termed the Korean permeability setup). The prismatic specimens were cracked in a three-point bending setup. Hence, the resulting crack geometry was triangular which is commonly found in structures subjected to bending loads. The cylindrical specimens were cracked in a Brazilian splitting setup. This method requires complete detachment of the two halves of the specimen in order to be able to insert silicone sheets which act as spacers. As such, this method cannot be used for liquid healing agents, that are often sequestered in macro- or microcapsules. In contrast, some studies have reported the use of the permeability test with prismatic specimens and active crack control for the evaluation of healing by microencapsulated agents [32-34]. Considering that the cylindrical specimens are split via a Brazilian splitting test, the resulting crack is uniform in width over the height of the specimens. This crack geometry can be found in structures subjected to shrinkage cracking or pure tensile loading. By employing both a permeability method with cracks of constant width, as well as triangular shaped bending cracks, any potential preference of crack healing in a particular case is considered.

The permeability method with cylindrical samples requires a shorter preparation time, allowing to prepare more specimens. On the other hand, the permeability method for prismatic specimens, gives more control due to the active crack width control. Furthermore, this method is more versatile, as the applied water pressure can be easily adapted. For the Korean permeability setup, one study has worked with a top reservoir with different overflow valves allowing the water head to be regulated with increments of 100 mm [35]. Nevertheless, the maximum water head was 500 mm, which is low compared to the maximum 2 bar which has been employed in the current study for the prismatic specimens. In case a higher variability on the crack width is accepted, the active crack width control can be swapped with a “passive” control technique for prismatic specimens by inserting tensile reinforcement or fibres and cracking the specimens with a crack-width controlled setup. This can be useful when working with liquid healing agents (e.g. in (micro)capsules) for which a controlled crack formation is desirable.

3.3.1. Prismatic specimens with active crack width control

The permeability test on prismatic specimens has been developed in a European collaboration project [36, 37]. An inter-laboratory test indicated that the variation on the crack widths of notched prismatic specimens was too high, resulting in inconclusive results with regards to the permeability [38]. In order to improve the test method, an active crack width control technique was developed [22]. The improved test method was studied again in an inter-laboratory test which concluded that the control of the crack width was essential for obtaining comparable permeability results, and that as such the permeability test for prismatic specimens with active crack width control has the potential for further standardization [33].

Six specimens were considered for each mix design (except for the WM series for which only five specimens were available). At an age of 28 days the prisms were cracked in a three-point bending setup (KU specimens were cracked at 27 days). At least one day prior to cracking a carbon fibre reinforced polymer (CFRP) strip was glued on the top of the specimens, which ensured that the specimen halves stayed together upon breaking (Figure 2). After removal of the load, the crack width was too large (order of magnitude of 1000 µm). To obtain the target crack width, the crack width was restrained using screw jacks. This was done under the microscope in order to accurately obtain a nominal crack width at the bottom of the specimens equal to 300 µm.

Once the crack width was restrained, aluminium tape was applied on the side of the specimens, ensuring that any water leaking from the crack would only come from the bottom side of the specimen. It has been noted that the active crack width control technique can result in a small closure of the crack which is not related to healing but is the result of an elastic regain in the CFRP and local creep and crushing of the mortar near the crack tip [22]. In order to limit the crack closure due to these phenomena and to fix the crack opening for the duration of the healing period, small CFRP strips were glued on the side of the specimen, see Figure 2.

The prismatic specimens were saturated overnight prior to measuring the initial flow rate $q_{initial}$. To measure the flow rate, the cast-in hole was slightly enlarged on one side to a diameter of 6 mm over a length of 2 cm. This allowed the insertion of a tube ($Ø_{outer}$ = 6 mm, $Ø_{inner}$ = 4 mm). A watertight connection was ensured with silicone which was also used to seal off the other side of the specimen. The tube was connected to the tubing of the water flow setup, inducing a constant water pressure of 50 cm water column. The water, flowing from the reservoir through the tubing into the specimen, leaked out through the crack mouth at the bottom side of the specimens, where it was captured in a container on an electronic measuring balance, see Figure 2.

After determining the initial flow rate, the specimens were immersed in water with their crack facing downwards. A separate container was used for each mix design. At 7, 14 and 28 days the specimens were taken out of the water container to determine the flow rate again. However, at 28 days it was noticed that the aluminium tape was detaching from the side of the specimens (especially when testing the specimens under high pressure, see following paragraph). Hence, the specimens were dried in lab conditions, the tape was removed and the sides were sealed again using epoxy coating. The specimens were saturated again and the final water flow q_{final} was determined. This allowed to determine the sealing efficiency:

$$SE = \frac{q_{initial} - q_{final}}{q_{initial}} \quad (1)$$

After determining the final water flow rate at 50 cm water head, the specimens were also subjected to a higher water pressure to verify the durability of the crack healing at higher pressure [18, 23]. The tube of the specimen was connected to a pressure vessel filled with water. The specimens were tested at 1 ± 0.1 bar and subsequently 2 ± 0.1 bar.

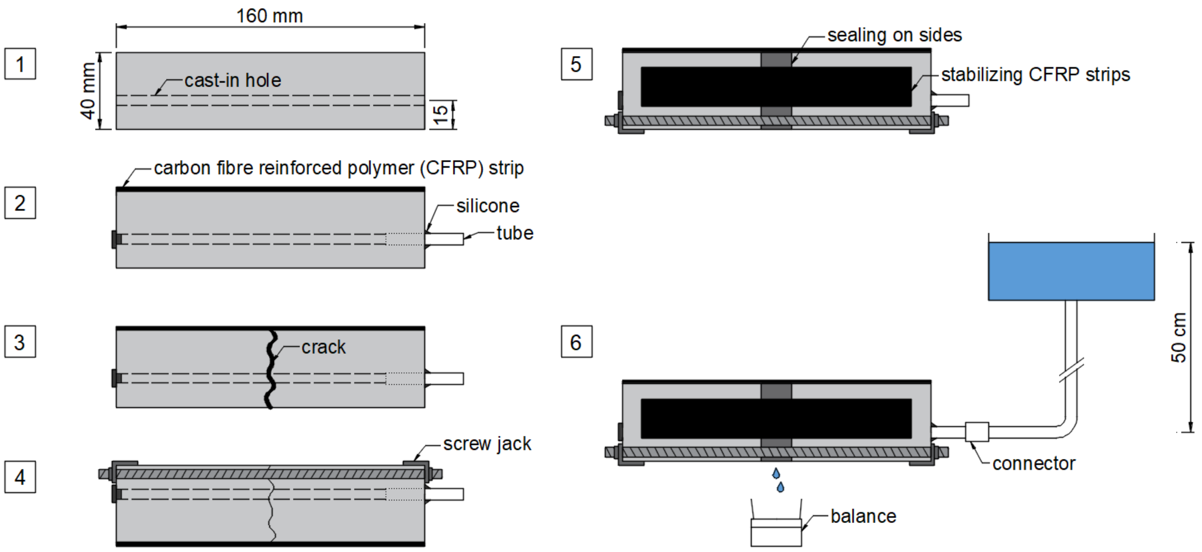

Figure 2. Schematic overview of the different steps of water permeability testing on prismatic specimens with active crack width control. (1) Prismatic mortar specimen 40 x 40 x 160 mm³ with cast-in hole at 15 mm from the bottom surface. (2) Gluing of CFRP strip on the top side (trowelling surface), insertion of tube after enlarging diameter of cast-in hole and ensuring water tightness with silicone. (3) Crack introduction via three-point bending setup. (4) Restraining of the crack with screw jacks (under the microscope). (5) Sealing of the side of the specimens and attaching CFRP strips on the sides to stabilize the crack. (6) Performing water permeability test by attaching the specimen to a reservoir inducing a water head of 50 cm and measuring the mass of the leaked water.

3.3.2. Cylindrical specimens (Korean permeability test method)

The permeability test for cylindrical specimens has been developed within the Self-Healing Green Concrete (SHGC) consortium; a Korea based consortium collaborating with dozens of researchers from different research institutes in Europe and Asia. This method has been thoroughly evaluated and employed for the evaluation of different healing agents [14, 15, 24, 25]. A guideline in Korean of this test method has been certified by the Korean Concrete Institute.

The cylindrical specimens were cracked at the age of 28 days via a Brazilian splitting test. Six specimens were considered for each mix design. After cracking, the two halves were put back together using hose clamps with silicon sheets with a nominal thickness of 300 µm between the two halves at the edges of the crack (Figure 3). Due to the silicon sheets the crack length was limited to 70 mm. After reassembling the cylinders, the crack width was measured using a microscope.

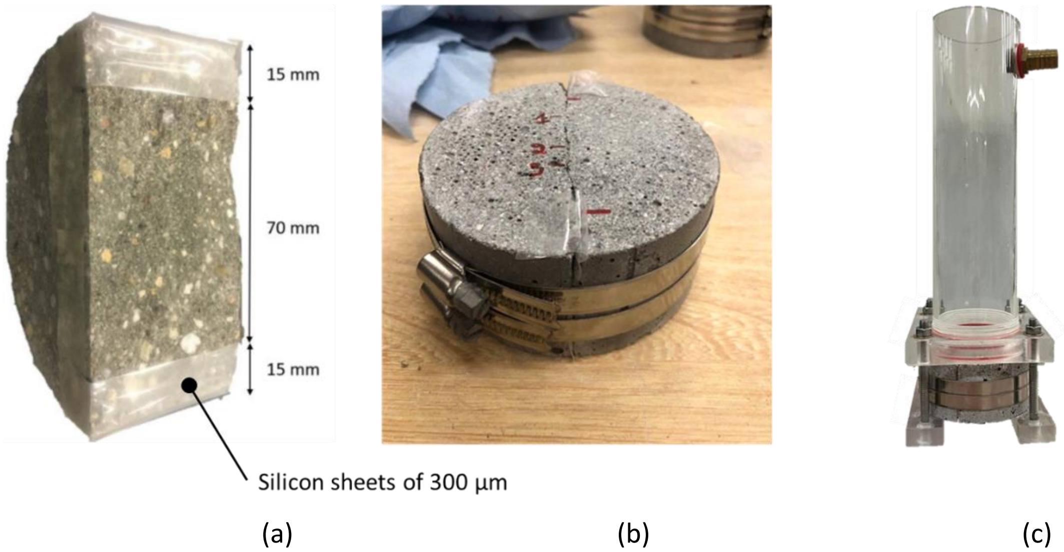

Figure 3: Overview of the preparation of the cylindrical specimens: (a) application of silicon sheets of 300 µm; (b) reassembled specimen with hose clamps; (c) cylindrical water reservoir attached on top of specimen.

The water permeability was tested on cracked cylindrical specimens using the Korean water permeability test. The flow rate $q_{initial}$ of the specimens was tested immediately after the cracking and reassembling of the sample. The described test method is based on the work of Shin et al. [24] and Lee et al. [25]. The (surface) dry specimen was placed between a Plexiglas plate with a circular hole of 63 mm at the top and two support bars at the bottom of the specimen, parallel with the crack. A rubber ring was placed between the plate and the top of the specimen to ensure a watertight connection. A cylindrical water reservoir with a height of 250 mm was attached on the top of the plate. Subsequently, the specimen was placed in a reservoir as such that the bottom of the specimen was just in contact with water. Then, the upper reservoir was filled with water and a constant overflow of the reservoir was ensured by a water supply of an external reservoir to obtain a constant water pressure. The water that flowed through the crack was collected in the lower reservoir and then flowed through an overflow in a container on an electronic measuring scale. After testing, the cylindrical specimens were placed with their longitudinal axis horizontally in a container so that the crack was immersed in water but the part of the specimens just above the crack was out of the water to promote healing. At 7, 14, 21 and 28 days, the specimens were taken out of the water 4 hours prior to testing the water permeability again. The sealing efficiency (SE) at time i, this is after 7, 14, 21 and 28 days of healing, could be calculated from $q_{initial}$ and the water flow at time i (q_i) as:

$$SE_i = \frac{q_{initial} - q_i}{q_{initial}} \quad (2)$$

3.4. Chloride diffusion

All three healing agents were tested in a chloride diffusion test. It has been reported that a regain in liquid tightness after crack healing does not necessarily guarantee impermeability with regards to the ingress of chloride ions [39]. For this reason a chloride diffusion test allows a deeper analysis for specimens with a good crack sealing.

After the final permeability test on the cylindrical specimens had been executed (after 28 days of healing), they were dried and subsequently coated (Episol Designtop SF, Resiplast, Belgium) except for the circular area that was placed as the top surface during the water permeability test. After the coating had dried, the specimens were saturated in water for 2 days. Subsequently, the specimens were placed in containers with a sodium chloride solution of 33 g/L. After 6, respectively 12 weeks, three cracked specimens of each set were taken out and opened along their crack and subsequently one half was split perpendicular to the crack plane. The two obtained pieces were sprayed with a 0.1 M silver nitrate solution to visualize the ingress of chloride ions perpendicular to the crack. The colour change boundary was marked, see Figure 4. Starting from the exposure surface, the chloride ingress perpendicular to the crack was determined every 5 mm over the height of the specimens, see horizontal lines in Figure 4. In addition, also the average depth of the colour change boundary in the uncracked zone (the zone not affected by the presence of the crack) was determined from four measurements with a spacing of 5 mm starting at 15 mm from the side of the specimens, see vertical dashed lines in Figure 4. For each series, there were also three uncracked specimens that were coated and placed in same the sodium chloride solution. They were taken out at 12 weeks and were split. On both halves 7 measurements of the depth of the colour change boundary were done (spacing of 10 mm starting at 20 mm from the side of the uncracked specimens).

Note that per split half the outliers were not considered when calculating the average depth of the colour change boundary in the uncracked zone. Outliers were defined as values being lower than the first quartile minus 1.5 times the interquartile range, respectively higher than the third quartile plus 1.5 times the interquartile range.

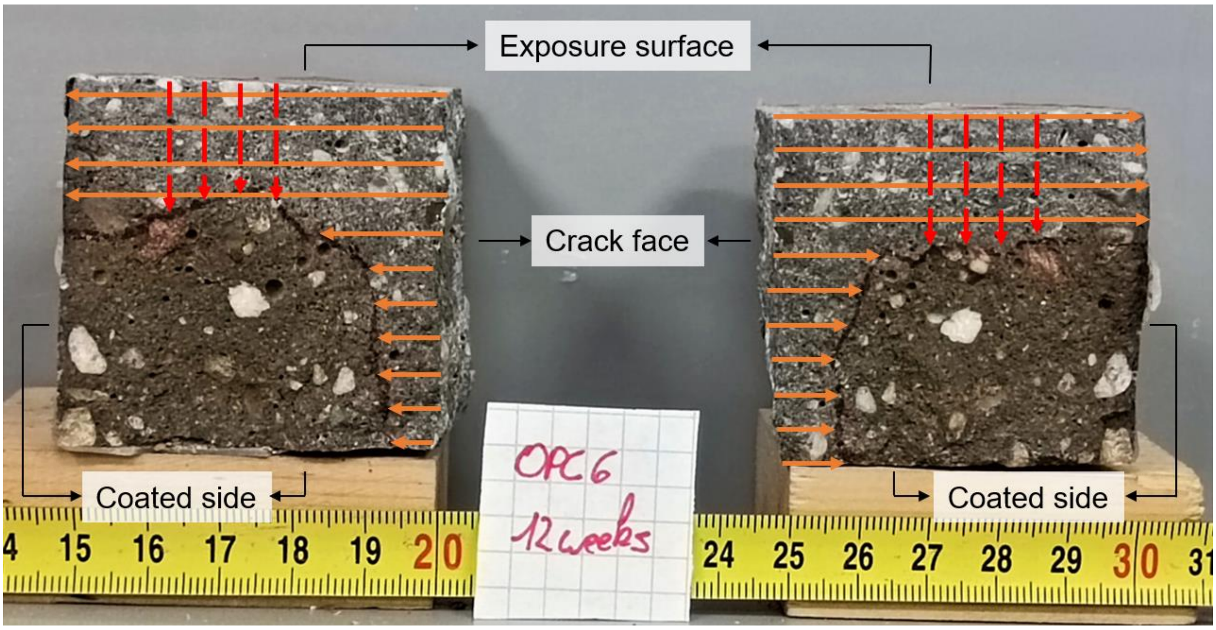

Figure 4: Example of measurement of colour change boundary in one of the REF specimens which was exposed for 12 weeks in the sodium chloride solution. The vertical dashed red arrows indicate the measurement of the "uncracked" zone. The horizontal full orange arrows show the measurement perpendicular to the crack wall starting from the exposure surface (top in the picture) toward the coated side (bottom in the picture).

3.5. Quasi-steady-state chloride migration test

In contrast to traditional methods employed in literature which use uncracked specimens, the quasi-steady-state method which was employed in this study has been specifically developed for cracked concrete [5, 40, 41]. A guideline (in Korean) has been certified by the Korean Concrete Institute. One interesting aspect of this method is that it is possible to record the performance for the same specimen as it is healing. This is impractical for diffusion testing as it requires splitting of the sample.

Two cracked specimens from the REF and WM mixtures were tested using a quasi-steady-state chloride migration method [5, 40]. Before starting the test, the specimens were vacuum saturated for at least 18 hours. The test method consisted of placing the specimens in a migration cell. The migration cell had an upstream and a downstream cell which were filled with a 0.5 M NaCl solution and a 0.3 M NaOH solution, respectively. For 24 hours, an electrical potential of 36 V was applied. In the last 8 hours, during the quasi-steady-state regime, the chloride concentration in the cell with NaCl solution was measured hourly and the chloride migration coefficient was determined. The chloride concentration in the upstream cell was measured by taking out a little bit of NaCl solution from the cell at regular time intervals and measuring the concentration with an Ion Selective Electrode (ISE). However, ISE electrodes can take some time to stabilize and even then still show quite some fluctuation, making an accurate assessment challenging and time-consuming.

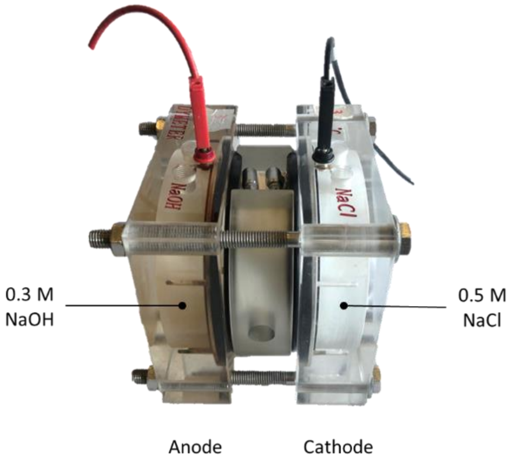

Figure 5: Setup chloride migration cell.

The specimens were tested after 0, 14, 28, 56 and 91 days of healing. To promote the healing in-between tests, they were placed in a container with the crack immersed in water, similar to the cylindrical specimens used for permeability testing. The KU and SMU healing agents were not developed for crack healing in chloride environments. Hence, they were not evaluated in this test.

The following adjustments were made to the test method to increase the performance and to decrease the variation on the results:

- The uncracked surface of the specimen was coated using an epoxy coating to increase the repeatability of the test as recommended by Yoo et al. [41] (Figure 6).
- The circumference of the cylinder was wrapped with Teflon tape before assembling the migration cell.
- The chloride concentration in the upstream cell was measured with an ISE using the following procedure: the ISE was brought into the test solution, then the solution was stirred for 30 seconds. After stirring, the ISE was left in the solution for 2 minutes after which the chloride concentration was read from the device.

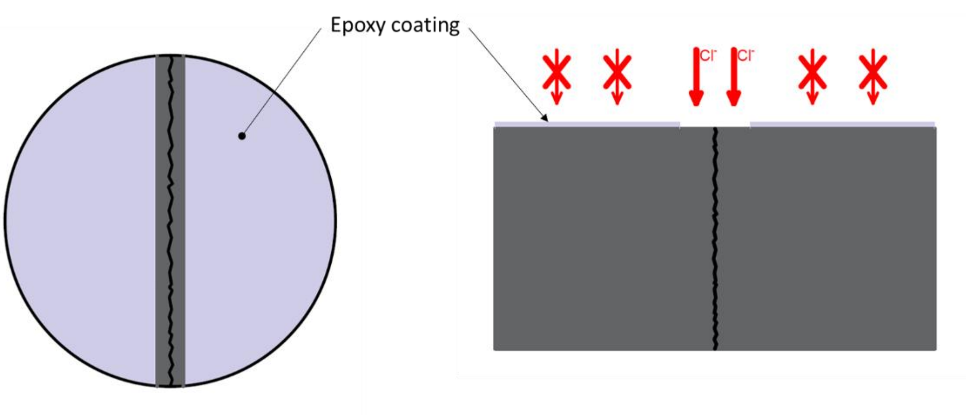

Figure 6: Epoxy coating on the uncracked surface of cracked cylindrical specimens.

3.6. Microscopic crack width measurement

The crack width was determined with a microscope camera (Leica DMC 2900). For the prismatic specimens, three images of the crack were taken at the bottom side of the specimens. On each image 5 measurements of the crack width were made, resulting in 15 measurements per sample. For the cylindrical specimens 6 images were taken on each side. On each image 2 measurements of the crack width were made, resulting in 24 measurements per sample.

4. Results

4.1. Fresh properties and strength

Table 2 gives the measured flow values of the fresh mortar mixtures. The flow for WM was significantly higher in comparison to KU, SMU and the reference mixture.

Table 2: Flow values of the fresh mixtures.

	Flow [mm]
REF	185
WM	225
SMU	145
KU	155

Figure 7 and Figure 8 show the flexural and compressive strength tested on mortar prisms (40 x 40 x 160 mm^3) at the age of 7 and 28 days. Regarding both flexural and compressive strength, the reference series performed best. An ANOVA analysis with a subsequent post-hoc Tukey test on the compressive strength results after 28 days showed that the means of WM and KU are significantly lower than REF and SMU (level of significance = 5 %, p < 2.7 %). An ANOVA analysis indicated that after 7 days the mean value for WM is significantly lower than the mean of REF and SMU (level of significance = 5 %, p < 4.3 %). However, there was no statistical difference found between the means of the different mixes after 28 days (level of significance = 5 %, minimum p = 32.1 %).

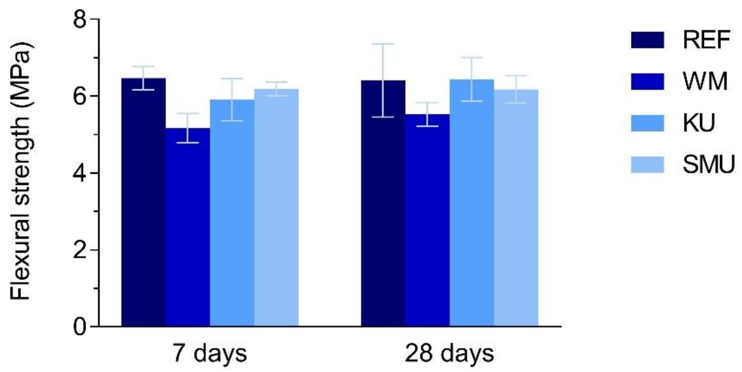

Figure 7: Flexural strength at the age of 7 and 28 days. Error bars represent the standard deviation.

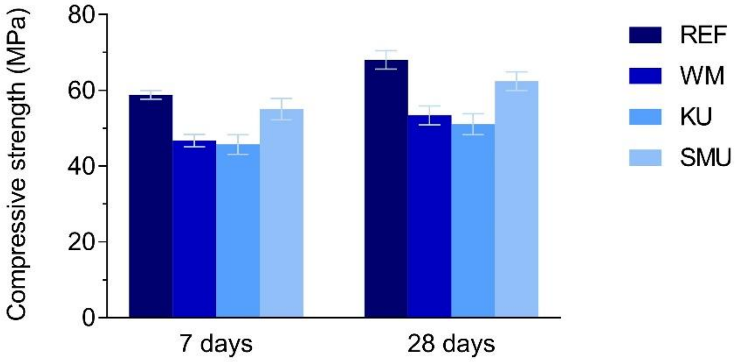

Figure 8: Compressive strength at the age of 7 and 28 days. Error bars represent the standard deviation.

4.2. Permeability testing on prismatic specimens with active crack width control

After cracking the prismatic specimens in a three-point bending setup, the crack widths were restrained with screw jacks under the microscope. Figure 9 shows the average crack width of the different prismatic specimens. For each series there were six specimens, except for the WM series for which one specimen failed during demoulding. An ANOVA analysis indicated the equality of the means of the different series (level of significance = 5%, p = 30.3%, equality of variances could be assumed with a level of significance = 1.0%, p = 74.3%). All series also obtained on average the intended crack width of 300 µm, as investigated by t-testing (level of significance = 5%, minimum p = 13,9%). In addition, it can be seen from Figure 9 that the standard deviation stays limited. In fact, the maximum standard deviation of the prismatic specimens (13 µm) is only half of that of the cylindrical specimens (26 µm), see section 4.3. This is a result of the active controlling of the crack width of the prismatic specimens with the screw jacks.

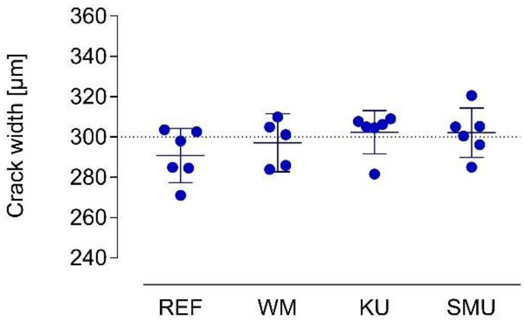

Figure 9. Crack width of the prismatic specimens. The mean of the different series is indicated by a horizontal line and the error bars give the 95% confidence interval.

The initial flow rate of the different specimens was compared to a theoretically calculated value based on the following regression formula [19, 22]:

$$q_{calc} = A \cdot w^3 \tag{3}$$

with q_{calc} the calculated flow rate (in g/min), w the mean crack width of a specimen (in m) and A a fitting constant. The value of the fitting constant can be assumed to be equal to 3.40E+12 for these types of specimens [22]. In case the measured initial flow rate diverged by more than 40% from the calculated flow rate, the specimen was withheld from further analysis. Figure 10 shows that one value of the REF, WM and KU series respectively fell outside of the postulated boundaries. From Table 3 it can be seen that, on average, the initial flow rate of the WM series is 10 g/min lower than that of the

REF series. This might be a result of the fast action of the expansive component of the WM healing agent, although it needs to be remarked that there is quite some spread on the flow data, despite the similar crack width, as can also be seen from Figure 10. This is to be expected; the variation on flow rates is an order of magnitude higher than the variation on crack widths [22].

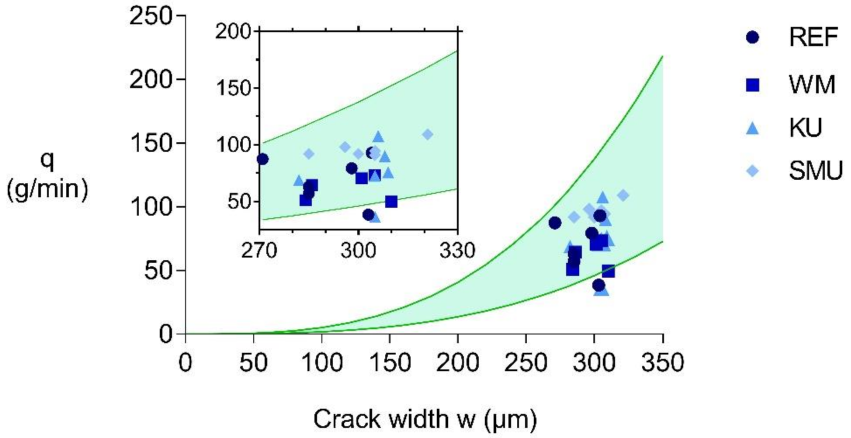

Figure 10. Measured initial flow rate q in function of mean crack width of the different prismatic specimens. The boundaries of the shaded area correspond to 60% q_{calc} and 140% q_{calc}.

After healing the specimens in saturated conditions the final water flow q_{final} could be determined, see Table 3. The WM series clearly performed best with a sealing efficiency of 100% (only one specimen had a limited flow of 0.01 g/min). Also the KU series performed well with an average sealing efficiency of 98% and two specimens with a sealing efficiency of a 100%. SMU performed worse with an average sealing efficiency of 87%, which was inferior to the REF which showed a SE of 94%. This is contradictory to previous research [15], in which the mix design also existed out of polyvinyl alcohol fibers, which could have served as a nucleation site. Overall, the REF healing was higher than in previous research [42]. The high crack sealing in the current study can be attributed to a high content of cement in the mix (sand-to-cement ratio of 2) and a relatively low water-to-cement ratio of 0.4. In fact, all series had some stalactite formation at the crack mouth, see Figure 11 a). At the end of the healing period it was found that the WM specimens showed longitudinal cracks, see Figure 11 b) and c). Most likely this is a result of the expansive action of the healing agent which was restrained by the screw jacks and CFRP plates. These cracks were sealed with epoxy coating in order to determine the final flow rate.

Table 3: Crack width w, initial and final flow rate q with a water head of 50 cm, and sealing efficiency SE of prismatic specimens. Light grey values were not taken into account when calculating the average which is shown in bold. NA: not available.

	w [µm]	$q_{initial}$ [g/min]	q_{final} [g/min]	SE
REF-1	303	38.34	1.81	95%
REF-2	285	62.92	0.88	99%
REF-3	285	57.00	4.86	91%
REF-4	298	79.17	0.04	100%
REF-5	271	87.32	6.63	92%
REF-6	304	92.95	10.26	89%
	288	**75.87**	**4.53**	**94%**

	w [µm]	$q_{initial}$ [g/min]	q_{final} [g/min]	SE
KU-1	306	107.62	1.22	99%
KU-2	305	36.43	0.60	98%
KU-3	308	89.80	2.41	97%
KU-4	282	68.87	0.00	100%
KU-5	305	72.53	3.72	95%
KU-6	309	75.60	0.00	100%
	302	**82.88**	**1.47**	**98%**

WM-1	310	49.68	0.00	100%
WM-2	301	70.42	0.01	100%
WM-3	284	50.98	0.00	100%
WM-4	305	73.30	NA	NA
WM-5	286	64.20	0.00	100%
	294	**64.73**	**0.00**	**100%**

SMU-1	321	109.07	14.77	86%
SMU-2	305	94.58	12.33	87%
SMU-3	305	90.87	1.51	98%
SMU-4	285	91.97	16.30	82%
SMU-5	300	91.85	19.84	78%
SMU-6	296	97.95	8.88	91%
	302	**96.05**	**12.27**	**87%**

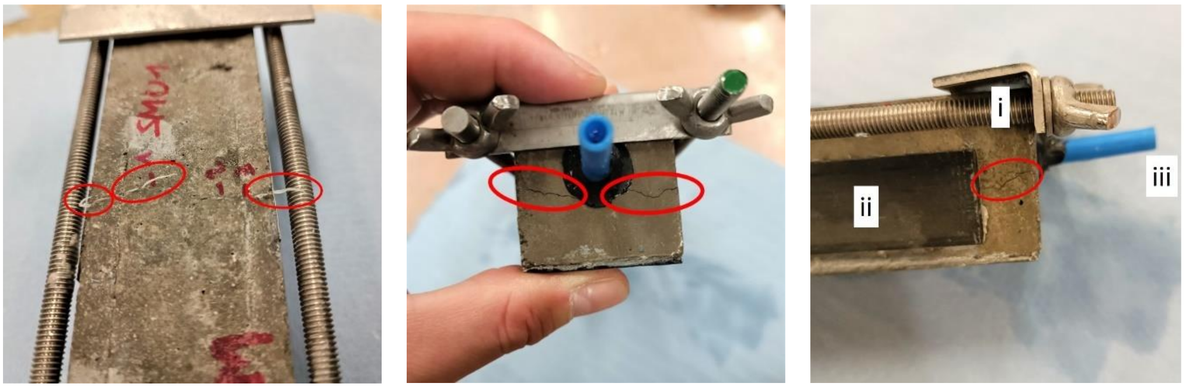

Figure 11: a) stalactite formation at the crack mouth for an SMU specimen, b) crack formation at end face of WM series; c) crack formation at side face of WM series with i) the screw jack used for active crack width control, ii) the small CFRP strip on the side to stabilize the specimen and iii) the tube which was inserted in the specimen to connect it to the water flow setup.

After measuring the final flow rate, the strength of the healing products was also tested by subjecting the specimens to a higher water pressure. Figure 12 shows the flow rate at 1 and 2 bar measured after recording the final flow rate at 50 cm water head (equivalent to ± 0.05 bar). The results of the specimens which were withheld due to the measured initial flow rate diverging too much from the theoretically calculated flow rate (see Figure 10) are not shown here. In case the flow rate was already high at 1 bar (> 80 g/min) the crack closure was deemed insufficient, and the specimen was not subjected to 2 bar. In such a case the plot just shows a flow of more than 100 g/min. It can be seen that the WM series performed best with only a small water flow (< 30 g/min) at 2 bar. Two out of the five KU specimens performed excellent at 2 bar keeping their water tightness which they had at a pressure of 0.05 bar (flow rate < 0.3 g/min). However, the other three which had a small water flow at 0.05 bar had a significant increase in flow rate at higher pressure. SMU performed worse than the REF, with five out of the six specimens having a flow of more than 100 g/min already at 1 bar, while none of the REF specimens had this flow at 1 bar.

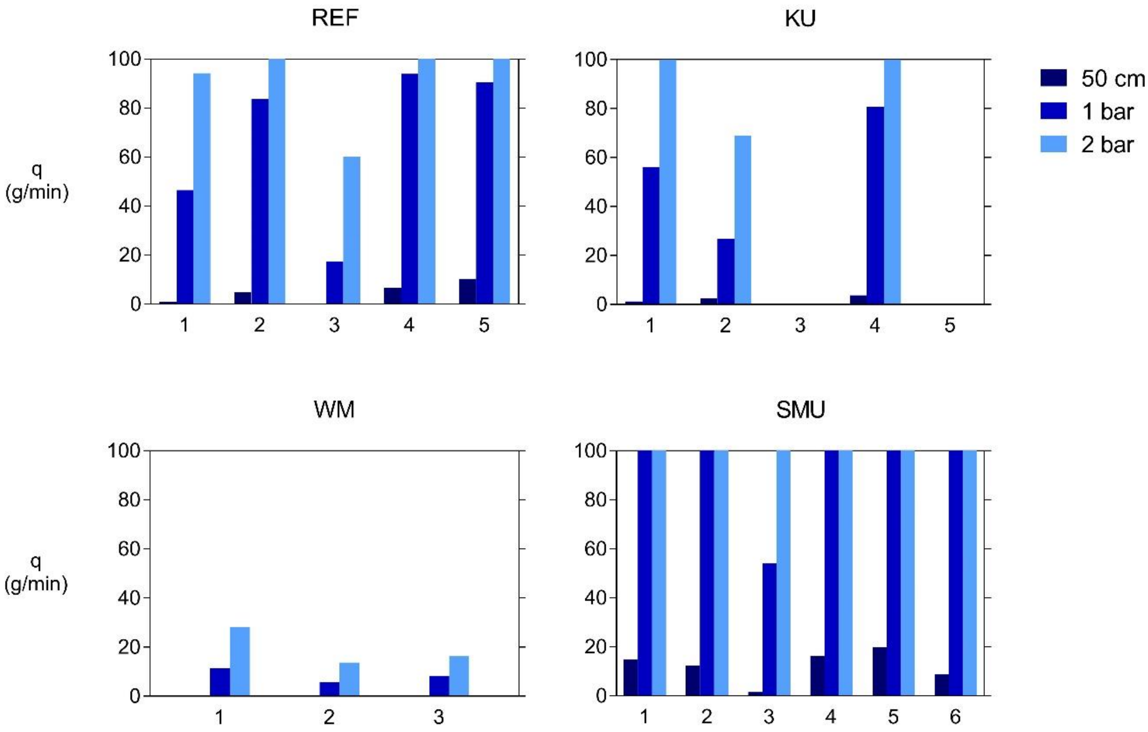

Figure 12. Comparison of the final water flow at 0.05 bar and the water flow at a high pressure of 1 and 2 bar.

Overall, for the prismatic specimens, which were healed completely immersed in water, the WM series performed consistently well, followed by the KU healing agent (with more variability). The addition of these healing agents showed a clear benefit with respect to the reference, as a result of the expansive action and the triggering of the bacteria for the WM and KU agent, respectively.

4.3. Permeability testing on cylindrical specimens

Figure 13 shows the average crack width of the different cylindrical specimens. An ANOVA analysis indicated the equality of the means of the different series (level of significance = 5%, p = 44.9%). All series also obtained on average the targeted crack width of 300 µm, as investigated by t-testing (level of significance = 5%, minimum p = 13,4%).

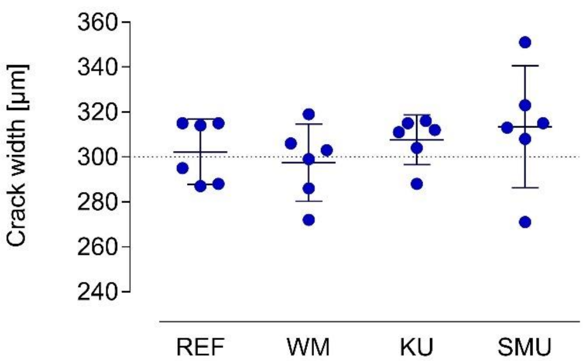

Figure 13: Crack width of the cylindrical specimens. The mean of the different series is indicated by a horizontal line and the error bars give the 95% confidence interval.

Figure 14 shows the sealing efficiency after 7, 14, 21 and 28 days of healing by putting half of the sample under immersion. The WM series performed best with a sealing efficiency of 78% after 28 days of healing, followed by REF with a sealing efficiency of 69% which can be attributed to the high content of cement in the mix. SMU and KU performed worse with a sealing efficiency of 64% and 43% respectively. The sealing efficiency of the KU series remained approximately the same after 14, 21 and 28 days. The significantly lower sealing efficiency for the cylindrical specimens in comparison to the prismatic specimens is possibly attributed to the orientation of the crack during immersion [43]. As previously described, the prismatic specimens were positioned with the crack mouth facing downwards. However, since the cylindrical specimens were placed with the crack horizontally, it was found that the formed healing products leaked out of the crack and were less optimal in clogging the crack mouth.

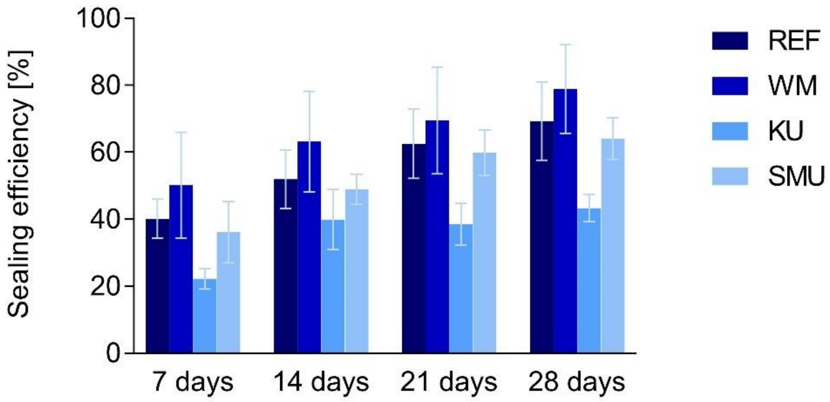

Figure 14: Sealing efficiency SE of first set of cylindrical specimens after 7, 14, 21 and 28 days of healing. Error bars represent the standard deviation.

The results obtained from this permeability test were lower than anticipated from previous research [14-16]. Therefore, the test was repeated with the exact same mix design, crack age and healing conditions, but with a different operator. The average crack width of the series was equal (level of significance = 5%, p = 13.3%). The results from this independent repetition are given in Figure 15**Fout! Verwijzingsbron niet gevonden.**. Overall these are more in line with the expectations from literature. It can be seen that the performance of the REF samples is lower; all series perform consistently better than the REF series at each time period. This confirms the results of the prismatic specimens; here the performance of SMU is even better as the prismatic SMU samples performed slightly worse than the prismatic REF samples. It can also be noted that the three cylindrical series with self-healing agents have a faster sealing than the REF, as they obtained the majority of their sealing earlier. The WM series performed best with an average sealing efficiency of 93% after 28 days of healing.

The exact reason for the diverging results of the first set are uncertain. Most likely the reproducibility was impaired since the first test was performed by a less experienced operator, which highlights the importance of a good training of the operator. It also needs to be remarked that the autogenous healing of the REF samples was relatively high. Yet, it has been remarked in literature that the autogenous healing behavior is rather scattered [2] and its reliability is questioned [44].

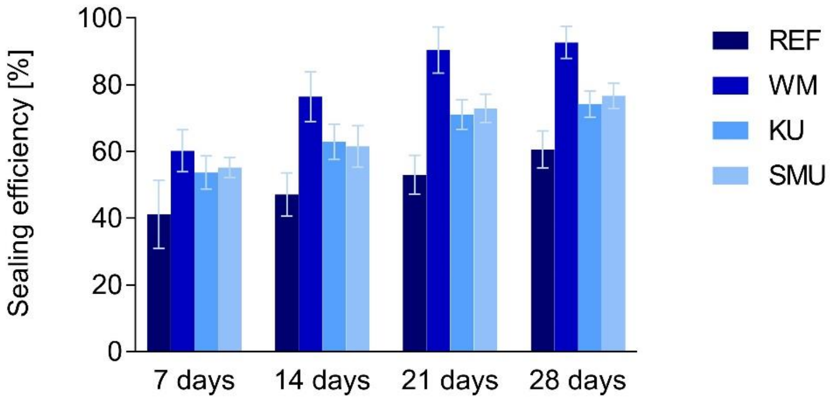

Figure 15: Sealing efficiency SE of second set of cylindrical specimens after 7, 14, 21 and 28 days of healing. Error bars represent the standard deviation.

4.4. Chloride diffusion

A chloride diffusion test was executed for 6 and 12 weeks. Figure 16 shows the depth of the colour change boundary in the uncracked zone. The results of 12 weeks are determined on uncracked specimens. The results of 6 weeks have been determined from the uncracked zone of cracked specimens, see section 3.4. Note that the pre-treatment of the cracked and uncracked specimens was the same. It is noted that the standard deviation for the WM series of 6 weeks is relatively large. This can be explained by the average of one specimen which was significantly larger than that of the other two specimens (17.6 mm compared to 13.1 mm and 12.8 mm). The figure indicates that the addition of the KU and SMU healing agents had a beneficial influence on the chloride ingress.

An ANOVA analysis did not show significant differences in the means for 6 weeks of exposure (level of significance = 5.0%, p = 11.2%, equality of variances could be assumed with a level of significance = 1.0%, p = 3.1%). However, for 12 weeks of exposure there were statistical differences (level of significance = 5.0%, p < 0.1%, equality of variances could be assumed with a level of significance = 1.0%, p = 11.5%). A Student-Newman-Keuls post hoc test defined three groups: SMU & KU < REF < WM (level of significance = 5%). However, a Tukey HSD (Honestly Significant Difference) post hoc test did not differentiate between the REF and KU series at 12 weeks (level of significance = 5.0%, p = 9.0%). Furthermore, it is remarked that the average colour change boundary at 12 weeks determined from the uncracked specimens was lower than the average determined in the uncracked zone of the cracked specimens (13.2 mm versus 15.0 mm). For the other three series the difference between the uncracked specimens and the uncracked zone of the cracked specimens was significantly lower (maximum difference of 0.6 mm).

Figure 17 and Figure 18 show the chloride ingress in the cracked specimens after 6 and 12 weeks respectively. The figures show the distance of the colour change boundary measured perpendicular to the crack wall (y-axis) versus the distance from the exposure surface (x-axis). For each exposure time and for each series three specimens were tested. The figures show the data markers of the two halves with the lines representing the average of a specimen. It can be seen that for several specimens the colour change boundary at the points the furthest away from the exposure surface (45 and 50 mm) is suddenly higher than in de middle of the specimen. This can be explained by some local crushing at the location of the crack on the circular section which was coated. Prior to coating, the crack was protected with a small strip of aluminium tape, preventing the epoxy coating to enter into the crack. This allowed some chloride solution to accumulate.

It is noted that the chloride diffusion was measured on the first series of cylindrical samples for water permeability and therefore provided conservative results. It is expected that the chloride ingress for KU and SMU would be lower than the results given in this section because of the higher sealing efficiency obtained on the second series of cylindrical samples.

After 6 weeks of exposure (Figure 17) the WM and REF series have a similar performance with at least one specimen having no significant chloride ingress perpendicular to the crack, i.e. the crack is sealed and the chloride ions have diffused in a way comparable to an uncracked specimen. For the KU and SMU there is still ingress along the crack. This is similar to the results of the Korean permeability setup (see section 4.3) where the highest sealing efficiency was obtained for the WM series.

After 12 weeks of exposure (Figure 18) the performance of the REF series was still quite good with two specimens having no significant ingress from the crack. However, one REF specimen had a significant ingress perpendicular to the crack. For two WM specimens there was no perpendicular ingress deeper down in the crack. Also considering the other WM specimen which was not optimally sealed, the ingress perpendicular to the crack remains lower than that of the poorly sealed REF specimen. Although it needs to be remarked that also from Figure 18 the poorer performance of the WM series with regards to diffusion in an uncracked state can be seen. Comparing Figure 17 and Figure 18 there is only a slight change in the KU series. Despite the non-optimal crack sealing of the KU series, as was also evident from the Korean water permeability results, the ingress of chloride ions goes slower than for the other series, like was also demonstrated from the chloride diffusion in the uncracked zone (Figure 16).

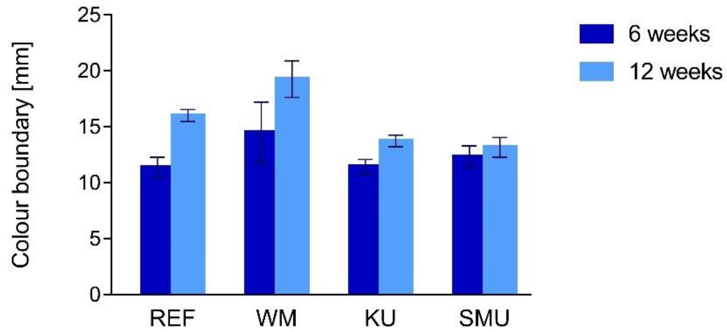

Figure 16. Depth of the colour change boundary in the uncracked zone. Error bars represent the standard deviation.

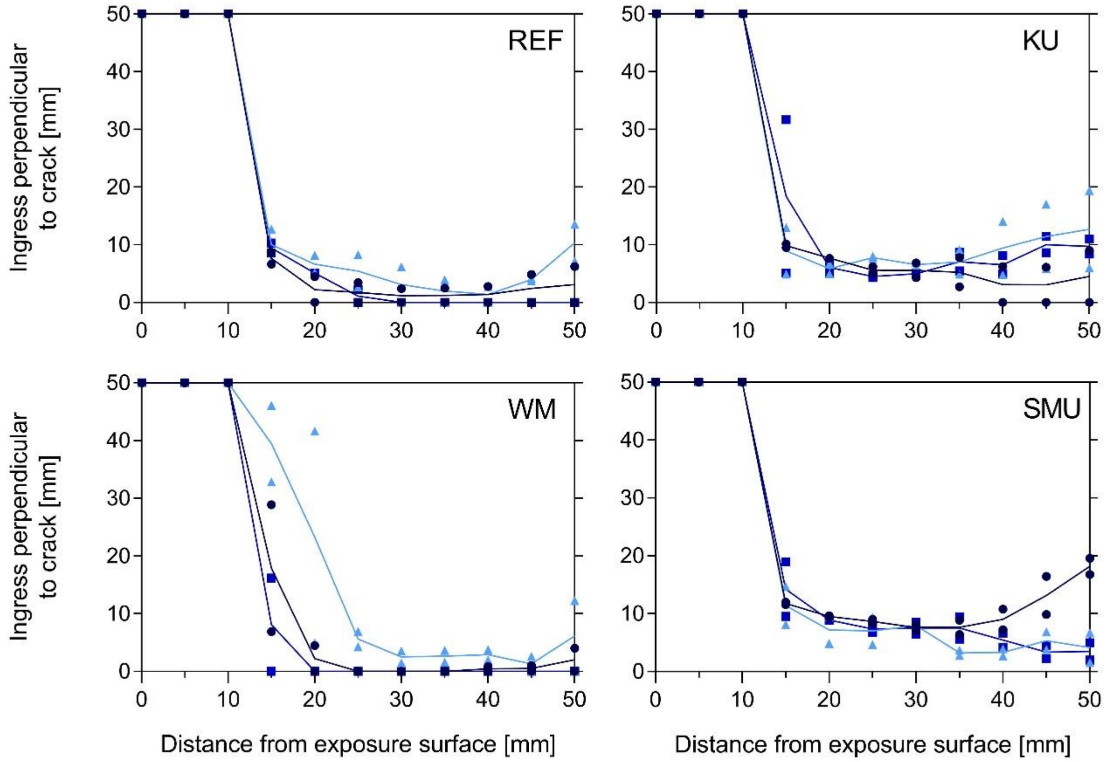

Figure 17. Chloride ingress perpendicular to crack after 6 weeks of exposure. Lines represent the mean of the two halves of a specimen.

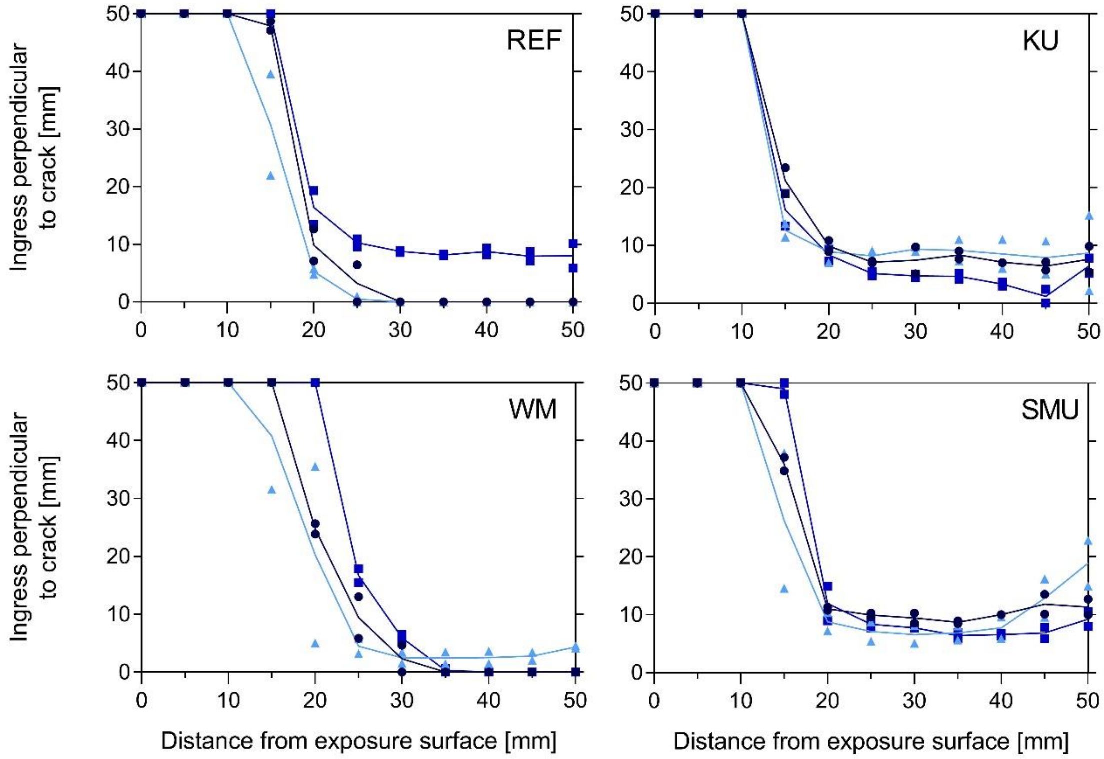

Figure 18. Chloride ingress perpendicular to crack after 12 weeks of exposure. Lines represent the mean of the two halves of a specimen.

4.5. Quasi-steady chloride migration test

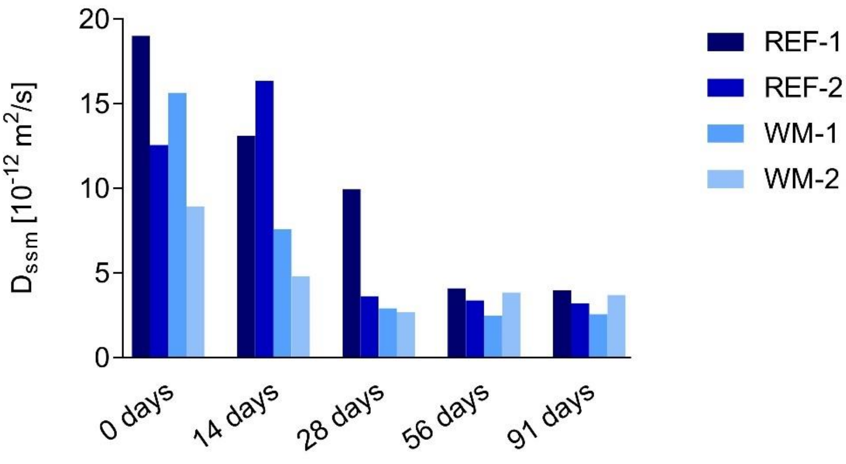

Figure 19: Chloride migration coefficient D_{ssm} of REF and WM specimens.

Figure 19 shows the migration coefficient of 2 cracked specimens of REF and WM after 0, 14, 28, 56 and 91 days of healing. After 14 and 28 days of healing, the addition of the healing agent WM leads to a decreased migration coefficient. After 56 and 91 days of healing, the difference between REF and WM becomes negligible. The precipitation of sodium chloride crystals inside and on the surface of the crack could lead to clogging of the crack and therefore a decreased chloride migration coefficient.

5. Discussion

The intent of this research is not to confirm a superior type of self-healing agent for concrete from all the developed healing agents available in literature. However, a comparison is made between the healing agents used in this research, and the best healing agent within this research is determined according to the calculated sealing efficiencies. The contribution of this paper is to study different types of healing agents with different tests to verify how the test method and the different boundary conditions affect the healing performance of the agents.

For both the water permeability test on prismatic specimens and the Korean water permeability test, WM (MgO-CaO in combination with an alkali activator) performed best with sealing efficiencies of respectively 100% and 93%. MgO and CaO, the main components of healing agent WM, have been frequently studied in literature as a healing agent. In literature, the addition of the expansive mineral additive MgO has shown to increase the healing efficiency of cracks [45, 46]. Qureshi and Al-Tabbaa found a complete closure of cracks up to 500 µm after 28 days of healing [47]. CaO has also proved to successfully seal cracks due to the formation of calcium hydroxide ($Ca(OH)_2$), which is able to react with CO_2 to form calcium carbonate $CaCO_3$ filling the cracks [48, 49]. The healing agent WM combined these 2 additives and the mechanochemical process was shown to increase the self-healing performance with 4.1 % [14]. The difference in sealing efficiency between the prismatic and cylindrical specimens obtained in this research shows that the crack geometry has a significant influence on the investigated healing performance. Therefore, it can be concluded that the healing efficiencies obtained with different methods should only be compared with extreme care. Furthermore, the chloride ingress through a crack also decreases with the use of WM as a healing agent as can be seen from the results of the chloride diffusion test (section 4.4) and the quasi-steady-state chloride migration test (section 4.5). However, the addition of WM to the mortar increases the chloride ingress in uncracked specimens up to 27% compared to the reference mix. It is noted that in previous literature the sealing efficiency was determined by water or gas permeability tests. This research also established that WM reduces the chloride ingress in cracks.

The performance of both SMU (capsules containing CSA and $CaSO_4$) and KU (pellets containing bacteria) depends on the used test method and the boundary conditions. For CSA and $CaSO_4$, sealing efficiencies in literature determined by a water flow test on samples with a uniform crack width over the height of the specimen are often higher in comparison to a reference mix [50, 51]. However, there are also studies available where the addition of CSA does not significantly increase the sealing efficiency [52]. This is in line with the results obtained in this research where SMU had a sealing efficiency of 87%, which is lower in comparison to the reference mix, where a sealing efficiency of 94% was obtained with the permeability test on prismatic specimens. However, regarding the Korean water permeability test, in the first test series SMU performed worse than the reference with a sealing efficiency of 64% compared to 69% for the reference. For the second test series, the sealing efficiency of SMU was 74%, which was higher than the 51% obtained for the reference. Regarding KU, the combination of *Lysinibacillus Boronitolerans* YS11 and *Bacillus Alkaliphilus* AK13, has been studied in literature as a healing agent. A higher sealing efficiency of the mix containing the non-pelletized bacteria in comparison to a reference mix was optically verified by studying the amount of healing product present in the crack [29]. The use of the bacterial pellets (KU) in literature increased the sealing efficiency quantified by a water permeability test on cylindrical specimens [16]. In this research, for the water permeability test on prismatic specimens, KU performed slightly better than the reference series with a sealing efficiency of 98% compared to 94% for the reference. Regarding the first series evaluated with the Korean water permeability test, KU performed worse than the reference with a sealing efficiency of 43% compared to 69% for the reference. In the second test series KU obtained a sealing efficiency of 77%, which was higher in comparison to a sealing efficiency of 51% for the reference. These findings also highlight the importance of a good training of the operator for the Korean water permeability test to ensure reliable and reproducible results.

6. Conclusion

The self-healing efficiency of WM, SMU and KU healing agents was compared in this research by using a low-head water flow test on prismatic specimens cracked in a three-point bending test with subsequent active crack width control, a Korean water permeability test on cylindrical specimens cracked by a Brazilian splitting test, a chloride diffusion test and a quasi-steady-state chloride migration test. The motivation for employing this set of test methods has been extensively explained with the hope of facilitating other comparative analyses.

The results showed that WM performed superior, not only with respect to the REF mix, but also with respect to the other healing agents. In both permeability setups the WM specimens showed high sealing efficiencies, in addition to a good performance with respect to the REF specimens in the quasi-steady-state chloride migration. Also in the chloride diffusion test the sealing of the crack of WM specimens was good with almost no chloride ingress from the crack into the matrix, perpendicular to the crack walls. However, in uncracked specimens, WM had the highest chloride ingress in comparison to the reference or the other healing agents. The performance of SMU and KU was depending on the healing condition. When healed in fully immersed conditions, the KU specimens showed a good behaviour with two specimens nearly maintaining perfect sealing even at 2 bar of water pressure. The SMU prisms performed poorly. However, for the second set of cylindrical specimens, where the crack was saturated but part of the specimen remained out of the water, SMU performed similar to KU and both of them performed better than the REF. Different results were obtained for the first set of cylindrical specimens, which were not in line with expectations from literature. Hence, it is underlined that operator sensitivity can influence results and that adequate training is necessary to counteract this.

Overall, the WM series performed best with regards to sealing efficiency for water tightness. In addition, the WM agent resulted in a reduced impact of cracks on the chloride ingress.

Acknowledgements

This research was supported by a grant (20SCIP-B103706-04) from the Construction Technology Research Program funded by the Ministry of Land, Infrastructure and Transport of the Korean government. Laurena De Brabandere wishes to thank the Research Foundation of Flanders (FWO) for the financial support on the research grant number 1SH8F24N.

References

[1] M. Pathak, R. Slade, P. R. Shukla, J. Skea, R. Pichs-Madruga, and D. Ürge-Vorsats, "Technical Summary," in *Climate Change 2022: Mitigation of Climate Change. Contribution of Working Group III to the Sixth Assessment Report of the Intergovernmental Panel on Climate Change*, P. R. Shukla *et al.* Eds. Cambridge, UK and New York, NY, USA: Cambridge University Press, 2022.

[2] N. De Belie *et al.*, "A review of self‐healing concrete for damage management of structures," *Advanced Materials Interfaces,* vol. 5, no. 17, p. 1800074, 2018, doi: https://doi.org/10.1002/admi.201800074.

[3] M. F. Montemor, A. M. P. Simões, and M. G. S. Ferreira, "Chloride-induced corrosion on reinforcing steel: from the fundamentals to the monitoring techniques," *Cement and Concrete Composites,* vol. 25, no. 4, pp. 491-502, 2003/05/01/ 2003, doi: https://doi.org/10.1016/S0958-9465(02)00089-6.

[4] P. Spiesz and H. J. H. Brouwers, "Influence of the applied voltage on the Rapid Chloride Migration (RCM) test," *Cement and Concrete Research,* vol. 42, no. 8, pp. 1072-1082, 2012/08/01/ 2012, doi: https://doi.org/10.1016/j.cemconres.2012.04.007.

[5] F. u. R. Abro, A. S. Buller, K.-M. Lee, and S. Y. Jang, "Using the steady-state chloride migration test to evaluate the self-healing capacity of cracked mortars containing crystalline, expansive, and swelling admixtures," *Materials,* vol. 12, no. 11, p. 1865, 2019.

[6] H. M. Jonkers, "Bacteria-based self-healing concrete," *In-Genium,* 2021.

[7] F. A. Gilabert, K. Van Tittelboom, J. Van Stappen, V. Cnudde, N. De Belie, and W. Van Paepegem, "Integral procedure to assess crack filling and mechanical contribution of polymer-based healing agent in encapsulation-based self-healing concrete," *Cement and Concrete Composites,* vol. 77, pp. 68-80, 2017/03/01/ 2017, doi: https://doi.org/10.1016/j.cemconcomp.2016.12.001.

[8] K. Van Tittelboom *et al.*, "Comparison of different approaches for self-healing concrete in a large-scale lab test," *Construction and Building Materials,* vol. 107, pp. 125-137, 2016/03/15/ 2016, doi: https://doi.org/10.1016/j.conbuildmat.2015.12.186.

[9] C. De Nardi, D. Gardner, and A. D. Jefferson, "Development of 3D Printed Networks in Self-Healing Concrete," *Materials*, vol. 13, no. 6*,* doi: 10.3390/ma13061328.

[10] Y. Shields, N. De Belie, A. Jefferson, and K. Van Tittelboom, "A review of vascular networks for self-healing applications," *Smart Materials and Structures,* vol. 30, no. 6, p. 063001, 2021.

[11] D. Snoeck, K. Van Tittelboom, S. Steuperaert, P. Dubruel, and N. De Belie, "Self-healing cementitious materials by the combination of microfibres and superabsorbent polymers," *Journal of Intelligent Material Systems and Structures,* vol. 25, no. 1, pp. 13-24, 2014, doi: https://doi.org/10.1177/1045389X12438623.

[12] M. Roig-Flores, S. Moscato, P. Serna, and L. Ferrara, "Self-healing capability of concrete with crystalline admixtures in different environments," *Construction and Building Materials,* vol. 86, pp. 1-11, 2015/07/01/ 2015, doi: https://doi.org/10.1016/j.conbuildmat.2015.03.091.

[13] L. Ferrara *et al.*, "Experimental characterization of the self-healing capacity of cement based materials and its effects on the material performance: A state of the art report by COST Action SARCOS WG2," *Construction and Building Materials,* vol. 167, pp. 115-142, 2018, doi: https://doi.org/10.1016/j.conbuildmat.2018.01.143.

[14] D.-C. Park, H. Kwon, J.-W. Lee, M.-Y. Hwang, and T.-H. Kim, "Performance Evaluation of Mortar Containing Mechanochemical Treated Self-Healing Admixtures," (in Korean), *Journal of the Korean Recycled Construction Resources Institute,* vol. 9, no. 3, pp. 367-374, 2021, doi: https://doi.org/10.14190/JRCR.2021.9.3.367.

[15] S.-R. Oh, K.-M. Lee, S. Choi, and Y.-W. Choi, "Fundamental Properties and Self-Healing Performance of Repair Mortar with Solid Capsules Made Using Inorganic Reactive Powder," *Materials,* vol. 15, no. 5, p. 1710, 2022, doi: https://doi.org/10.3390/ma15051710.

[16] I. Jang, D. Son, Y. Son, J. Min, and C. Yi, "Use of Methylcellulose-Based Pellet to Enhance the Bacterial Self-Healing of Cement Composite," *Materials,* vol. 14, no. 20, p. 6113, 2021, doi: https://doi.org/10.3390/ma14206113.

[17] G. Lefever, D. Snoeck, D. G. Aggelis, N. De Belie, S. Van Vlierberghe, and D. Van Hemelrijck, "Evaluation of the Self-Healing Ability of Mortar Mixtures Containing Superabsorbent Polymers and Nanosilica," *Materials,* vol. 13, no. 2, p. 380, 2020, doi: https://doi.org/10.3390/ma13020380.

[18] E. Gruyaert *et al.*, "Self-healing mortar with pH-sensitive superabsorbent polymers: testing of the sealing efficiency by water flow tests," *Smart Materials and Structures,* vol. 25, no. 8, p. 084007, 2016, doi: https://doi.org/10.1088/0964-1726/25/8/084007.

[19] C. Edvardsen, "Water permeability and autogenous healing of cracks in concrete," *Materials Journal,* vol. 96, no. 4, pp. 448-454, 1999.

[20] B. Van Belleghem, K. Van Tittelboom, and N. De Belie, "Efficiency of self-healing cementitious materials with encapsulated polyurethane to reduce water ingress through cracks," *Materiales de Construcción,* vol. 68, no. 330, 2018, doi: https://doi.org/10.3989/mc.2018.05917.

[21] L. De Brabandere, T. Van Mullem, N. Alderete, D. Baeyens, and N. De Belie, "Influencing factors to the capillary water uptake of (un)cracked cementitious materials," *MATEC Web Conf.,* vol. 378, p. 02028, 2023, doi: https://doi.org/10.1051/matecconf/202337802028.

[22] T. Van Mullem, E. Gruyaert, B. Debbaut, R. Caspeele, and N. De Belie, "Novel active crack width control technique to reduce the variation on water permeability results for self-healing concrete," *Construction and Building Materials,* vol. 203, pp. 541-551, 2019, doi: https://doi.org/10.1016/j.conbuildmat.2019.01.105.

[23] T. Van Mullem, R. Caspeele, and N. De Belie, "The influence of SAPs on chloride ingress in cracked concrete," in *Concrete Solutions 2019 – 7th International Conference on Concrete Repair* Cluj Napoca, Romania, M. G. Grantham and C. Mircea, Eds., 30 September - 2 October 2019 2019, vol. 289, no. MATEC Web of Conferences: EDP Sciences, 2019, p. 08007, doi: https://doi.org/10.1051/matecconf/201928908007

[24] K. J. Shin, W. Bae, S.-W. Choi, M. W. Son, and K. M. Lee, "Parameters influencing water permeability coefficient of cracked concrete specimens," *Construction and Building Materials,* vol. 151, pp. 907-915, 2017/10/01/ 2017, doi: https://doi.org/10.1016/j.conbuildmat.2017.06.093.

[25] K.-M. Lee, H.-S. Kim, D.-K. Lee, and K.-J. Shin, "Self-Healing Performance Evaluation of Concrete Incorporating Inorganic Materials Based on a Water Permeability Test," *Materials,* vol. 14, no. 12, p. 3202, 2021. [Online]. Available: https://www.mdpi.com/1996-1944/14/12/3202.

[26] J. Zhang, "Recent advance of MgO expansive agent in cement and concrete," *Journal of Building Engineering,* vol. 45, p. 103633, 2022/01/01/ 2022, doi: https://doi.org/10.1016/j.jobe.2021.103633.

[27] T. S. Qureshi, A. Kanellopoulos, and A. Al-Tabbaa, "Encapsulation of expansive powder minerals within a concentric glass capsule system for self-healing concrete," *Construction and Building Materials,* vol. 121, pp. 629-643, 2016/09/15/ 2016, doi: https://doi.org/10.1016/j.conbuildmat.2016.06.030.

[28] M. Sopicka-lizer, "1 - Introduction to mechanochemical processing," in *High-Energy Ball Milling*, M. Sopicka-Lizer Ed.: Woodhead Publishing, 2010, pp. 1-5.

[29] I. Jang, D. Son, W. Kim, W. Park, and C. Yi, "Effects of spray-dried co-cultured bacteria on cement mortar," *Construction and Building Materials,* vol. 243, p. 118206, 2020/05/20/ 2020, doi: https://doi.org/10.1016/j.conbuildmat.2020.118206.

[30] *Methods of test for mortar for masonry - Part 3: Determination of consistence of fresh mortar (by flow table)*, NBN, Brussels, Belgium, 2007.

[31] *Methods of testing cement - Part 1: Determination of strength*, NBN, Brussels, Belgium, 2016.

[32] G. Anglani *et al.*, "Sealing efficiency of cement-based materials containing extruded cementitious capsules," *Construction and Building Materials,* vol. 251, p. 119039, 2020/08/10/ 2020, doi: https://doi.org/10.1016/j.conbuildmat.2020.119039.

[33] T. Van Mullem *et al.*, "Addressing the need for standardization of test methods for self-healing concrete: an inter-laboratory study on concrete with macrocapsules," *Science and Technology of Advanced Materials,* vol. 21, no. 1, pp. 661-682, 2020, doi: https://doi.org/10.1080/14686996.2020.1814117.

[34] T. Van Mullem, K. Van Tittelboom, E. Gruyaert, R. Caspeele, and N. De Belie, "Development of an improved cracking method to reduce the variability in testing the healing efficiency of self-healing mortar containing encapsulated polymers," in *International Conference on Concrete Repair, Rehabilitation and Retrofitting (ICCRRR2018)*, Cape Town, South Africa, M. Alexander, H. Beushausen, F. Dehn, and P. Moyo, Eds., 19-21 November 2018 2018, vol. 199, no. MATEC Web of Conferences: EDP Sciences, pp. 1-5, doi: https://doi.org/10.1051/matecconf/201819902017.

[35] G. Hong, J. Kim, S. Oh, C. Song, and S. Choi, "Effect of crack widths and water pressures on crack sealing behavior of cementitious materials incorporating spherical superabsorbent polymers," *Construction and Building Materials,* vol. 300, p. 124219, 2021.

[36] E. Tziviloglou, V. Wiktor, H. Jonkers, and E. Schlangen, "Bacteria-based self-healing concrete to increase liquid tightness of cracks," *Construction and Building Materials,* vol. 122, pp. 118-125, 2016, doi: http://dx.doi.org/10.1016/j.conbuildmat.2016.06.080.
[37] E. Tziviloglou, H. M. Jonkers, and E. Schlangen, "Bacteria-based Self-Healing Concrete to Increase Liquid Tightness of Cracks," presented at the First conference on ageing of materials and structures, Delft, The Netherlands, 2014.
[38] E. Tziviloglou *et al.*, "Evaluation of experimental methodology to assess the sealing efficiency of bacteria-based self-healing mortar: round robin test," in *RILEM Conference on Microorganisms-Cementitious Materials Interactions*, Delft, the Netherlands, V. Wiktor, E. Schlangen, and A. Bertron, Eds., 23 June 2016 2016, vol. 102: RILEM, 2016, pp. 156-170.
[39] C. Litina *et al.*, "Evaluation of Methodologies for Assessing Self-Healing Performance of Concrete with Mineral Expansive Agents: An Interlaboratory Study," *Materials,* vol. 14, no. 8, p. 2024, 2021. [Online]. Available: https://www.mdpi.com/1996-1944/14/8/2024.
[40] F. u. R. Abro *et al.*, "Autogenous Healing of Cracked Mortar Using Modified Steady-State Migration Test against Chloride Penetration," *Sustainability,* vol. 13, no. 17, p. 9519, 2021. [Online]. Available: https://www.mdpi.com/2071-1050/13/17/9519.
[41] K. S. Yoo, S. Y. Jang, and K.-M. Lee, "Recovery of Chloride Penetration Resistance of Cement-Based Composites Due to Self-Healing of Cracks," *Materials*, vol. 14, no. 10*,* doi: 10.3390/ma14102501.
[42] E. Tziviloglou, V. Wiktor, H. M. Jonkers, and E. Schlangen, "Bacteria-based self-healing concrete to increase liquid tightness of cracks," *Construction and Building Materials,* vol. 122, pp. 118-125, 2016.
[43] T. Van Mullem, E. Gruyaert, R. Caspeele, and N. De Belie, "First Large Scale Application with Self-Healing Concrete in Belgium: Analysis of the Laboratory Control Tests," *Materials,* vol. 13, no. 4, p. 997, 2020, doi: https://doi.org/10.3390/ma13040997.
[44] L. M. Mauludin and C. Oucif, "Modeling of self-healing concrete: A review," *Journal of Applied and Computational Mechanics,* vol. 5, no. Special Issue: Computational Methods for Material Failure, pp. 526-539, 2019, doi: https://doi.org/10.22055/jacm.2017.23665.1167.
[45] B. Saleh Salem Beshr, I. M. Abdul Mohaimen, M. N. Noor Azline, S. Nor Azizi, A. B. Nabilah, and A. A. Farah Nora Aznieta, "Feasibility assessment on self-healing ability of cementitious composites with MgO," *Journal of Building Engineering,* vol. 34, p. 101914, 2021/02/01/ 2021, doi: https://doi.org/10.1016/j.jobe.2020.101914.
[46] M. Amenta, S. Papaioannou, V. Kilikoglou, and I. Karatasios, "Morphological and Chemical Characterization of Self-Healing Products in MgO Concrete," in *Proceedings of the 3rd RILEM Spring Convention and Conference (RSCC 2020)*, Cham, J. Sena-Cruz, L. Correia, and M. Azenha, Eds., 2022// 2022: Springer International Publishing, pp. 335-348.
[47] T. Qureshi and A. Al-Tabbaa, "Self-healing of drying shrinkage cracks in cement-based materials incorporating reactive MgO," *Smart Materials and Structures,* vol. 25, no. 8, p. 084004, 2016.
[48] M. Seifan, A. K. Samani, and A. Berenjian, "Bioconcrete: next generation of self-healing concrete," *Applied Microbiology and Biotechnology,* vol. 100, no. 6, pp. 2591-2602, 2016/03/01 2016, doi: 10.1007/s00253-016-7316-z.
[49] K. Van Tittelboom and N. De Belie, "Self-Healing in Cementitious Materials—A Review," *Materials*, vol. 6, no. 6*,* pp. 2182-2217doi: 10.3390/ma6062182.
[50] N. De Belie *et al.*, "A review of self‐healing concrete for damage management of structures," *Advanced materials interfaces,* vol. 5, no. 17, p. 1800074, 2018.
[51] B. Park and Y. C. Choi, "Quantitative evaluation of crack self-healing in cement-based materials by absorption test," *Construction and Building Materials,* vol. 184, pp. 1-10, 2018/09/30/ 2018, doi: https://doi.org/10.1016/j.conbuildmat.2018.06.206.
[52] B. Park and Y. C. Choi, "Effect of healing products on the self-healing performance of cementitious materials with crystalline admixtures," *Construction and Building Materials,* vol. 270, p. 121389, 2021/02/08/ 2021, doi: https://doi.org/10.1016/j.conbuildmat.2020.121389.